Quantification of CO$_2$ uptake by enhanced weathering of silicate minerals applied to acidic soils

Christiana Dietzen [a,b,*], Minik T. Rosing [a]

[a] Globe Institute, University of Copenhagen, Øster Voldgade 5-7, 1350 Copenhagen K, Denmark
[b] Geological Survey of Denmark and Greenland, Øster Voldgade 10, 1350 Copenhagen K, Denmark

ARTICLE INFO

ABSTRACT

The application of ground silicate minerals to agricultural soils has been proposed as a method for taking up CO$_2$ by enhancing the weathering rate of these minerals through their exposure to soil acids. Alternatively, glacial rock flour, a finely grained material which is abundantly available without the need for energy-intensive grinding, could be used. However, simple and inexpensive methods for determining the amount of CO$_2$ taken up as a result of weathering of applied minerals are still needed, and the impact of non-carbonic acids on CO$_2$ uptake has yet to be accounted for. Here, we present a protocol for correcting estimates of CO$_2$ uptake due to enhanced mineral weathering to account for weathering by non-carbonic soil acids. We determine that soils with a pH below 6.3 need correction for weathering by other acids than carbonic acid and that, given the impact of non-carbonic acids, soils with a pH below 5.2 may not be ideal candidates for mineral applications aimed at CO$_2$ uptake, depending on the pCO$_2$. We report an estimated CO$_2$ uptake of 728 kg CO$_2$ ha^{-1} after the application of 50 tons ha^{-1} of Greenlandic glacial rock flour to an acidic, sandy soil in Denmark over 3 years.

1. Introduction

According to the IPCC's 2018 report, negative emissions technologies are now necessary to prevent >1.5 °C of global warming (IPCC, 2018). Recently, the enhanced weathering of silicate minerals through application to agricultural lands has gained traction as a possible tool for sequestering significant amounts of carbon and improving agricultural productivity in highly weathered and nutrient depleted soils (Amann and Hartmann, 2019; Beerling et al., 2018; Haque et al., 2019; Kelland et al., 2020). The dissolution of silicate minerals by carbonic acid consumes H^+ ions and releases base cations, which allows for the dissociation of dissolved CO$_2$ to bicarbonate and carbonate ions (carbonate alkalinity), sequestering CO$_2$ as dissolved inorganic carbon. These weathering products may eventually be transported to the ocean where they can be stored for thousands of years (Renforth and Henderson, 2017).

This process has a number of potential co-benefits, namely counteracting ocean acidification by contributing alkalinity and improving crop yields via the release of plant nutrients (Hartmann et al., 2013). Selling carbon credits based on the CO$_2$ consumed could offset the cost of the mineral applications, but quantifying the amount of CO$_2$ taken up by mineral dissolution in such a way that fulfills the requirements of carbon accreditation agencies without incurring high measurement costs can be difficult (Amann and Hartmann, 2022). Though it is possible to measure the increase in pedogenic carbonate in alkaline soils (Haque et al., 2020; Khalidy et al., 2021), methodologies that can be used by farmers have not yet been developed for acidic soils, which comprise over half of the world's potentially arable land (Von Uexkull and Mutert, 1995).

Here we develop a method of calculating CO$_2$ uptake from silicate weathering that also corrects for weathering by sources of acidity other than carbonic acid, which would decrease the amount of carbon uptake associated with mineral weathering. This method is based on differences in soil exchangeable cations (Mg^{2+}, Ca^{2+}, K$^+$, and Na$^+$ held by negative charges on the soil surface) as a proxy for dissolution. Though this method is applicable to the application of any form of silicate minerals, we demonstrate its use with data taken over the course of 3 years from a field trial with the application of glacial rock flour from Greenland to a sandy agricultural soil in southern Denmark. We show that Greenlandic glacial rock flour, which has been shown to significantly improve crop yields (Gunnarsen et al., 2023), can also be effectively used to take up CO$_2$ through enhanced weathering.

---

* Corresponding author.
*E-mail address:* christiana.dietzen@sund.ku.dk (C. Dietzen).

1.1. Methods for quantification of CO_2 consumption

Placing silicate minerals in the soil environment allows the weathering action of soil acids, including carbonic acid, to increase the rate of mineral dissolution (Harley and Gilkes, 2000). The decomposition of organic matter can elevate the soil pCO_2 up to 100 times relative to the atmosphere (Strawn et al., 2015). Elevated pCO_2 increases the concentration of carbonic acid in the soil solution, which can react with silicate minerals to release base cations and generate alkalinity, as illustrated by the dissolution of the feldspar anorthite:

$$CaAl_2Si_2O_8 + 2H_2CO_3 + H_2O \rightarrow Ca^{2+} + 2HCO_3^- + Al_2Si_2O_5(OH)_4 \quad (1)$$
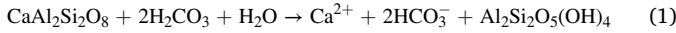
Organic acids in the soil can also be important drivers of mineral dissolution via ligand-promoted release of Al from the crystal lattice. The dissolution of the Al-Si framework can be the rate-limiting step in the dissolution process, which indirectly affects the rate at which cations can be released by proton-promoted dissolution by carbonic and other inorganic acids (Welch and Ullman, 1993). Weathering with carboxylic acids would also lead to increased alkalinity and potentially CO_2 uptake and export from soils.

Given the complexity of factors affecting the weathering process, it is currently not possible to accurately predict weathering rates of a specific mineral applied to a specific location over time. It is therefore necessary that methods for measuring the amount of CO_2 that has been taken up in the years following silicate mineral applications be developed so that farmers can profit from the sale of carbon credits.

If all of the silicate mineral dissolution in the soil were due to carbonic acid, carbon uptake could easily be calculated based on the difference in soil exchangeable cations relative to a control as a proxy for mineral weathering if we can make the assumption that these cations will be flushed out of the system rather than re-precipitated or taken up by plants at a later date. However, when stronger acids are present in the soil, weathering may be more rapid, but the total consumption of CO_2 can be significantly diminished due to weathering by other sources of acidity, which does not generate carbonate alkalinity (Taylor et al., 2021).

$$K_1 = \frac{[H^+][HCO_3^-]}{[H_2CO_3]} \quad (2)$$

by rearranging to solve for

$$[HCO_3^-] = \frac{K_1 \times [H_2CO_3]}{[H^+]} \quad (3)$$

To determine the amount of H_2CO_3 converted to HCO_3^- during mineral dissolution, we must calculate the value of a correction factor, X, that represents the proportion of the weathering reactions that converted carbonic acid to bicarbonate rather than consuming excess acidity. The new concentrations of HCO_3^- and H^+ would therefore be calculated as follows, wherein t_1 indicates the initial concentrations before mineral weathering, t_2 indicates concentrations after weathering, and M indicates the moles of positive charge released by weathering based on soil cation measurements:

$$\left[HCO_{3\ t_2}^-\right] = \left[HCO_{3\ t_1}^-\right] + (M \times X) \quad (4)$$

and, given that only the portion of weathering reactions that do not generate carbonate alkalinity will consume excess protons in the soil solution,

$$\left[H_{t_2}^+\right] = \left[H_{t_1}^+\right] - M \times (1-X) \quad (5)$$

Given that:

$$K_1 \times [H_2CO_3] = \left[HCO_{3\ t1}^-\right]\left[H_{t1}^+\right] = \left[HCO_{3\ t2}^-\right]\left[H_{t2}^+\right] \quad (6)$$

$$= \left[\left[HCO_{3\ t1}^-\right] + (M \times X)\right]\left[\left[H_{t1}^+\right] - M \times (1-X)\right]$$

$$= \left[\frac{K_1 \times [H_2CO_3]}{[H_{t1}^+]} + M \times X\right] \times \left[\left[H_{t1}^+\right] - M \times (1-X)\right]$$

We can calculate X as following given the initial (t_1) pH and pCO_2 of a soil solution (S1: Equation Derivation):

$$X = \left\{M^2 - \left[\frac{M \times K_1 \times [H_2CO_3]}{[H^+]}\right] - M \times [H^+] + \sqrt{\left[\frac{M \times K_1 \times [H_2CO_3]}{[H^+]} + M \times [H^+] - M^2\right]^2 + \frac{4 \times M^3 \times K_1 \times [H_2CO_3]}{[H^+]}}\right\} \div 2M^2 \quad (7)$$

Measuring differences in carbonate alkalinity output would correctly reflect the amount of carbon uptake, but this requires collecting soil porewater or leachate, which is a difficult process that is unlikely to be undertaken by the farmers who might use silicate minerals on their fields and hope to earn carbon credits. We have therefore developed a function that uses soil pH and pCO_2 to correct the calculated carbon uptake based on differences in exchangeable cations in soil samples, which farmers are accustomed to taking, to account for alternative sources of acidity.

Here we develop a formula to calculate what percentage of the maximum potential CO_2 uptake due to weathering has occurred as a function of the initial soil pH and pCO_2. In acid soils, dissolved inorganic carbon remains primarily in the form of bicarbonate and $H_2CO_3^*$. Given the soil pH and pCO_2, and assuming the pCO_2 remains constant as in an open system, we can determine the HCO_3^- in the soil solution via the formula for the equilibrium constant of carbonate systems, where $[H_2CO_3]$ = pCO_2 (atm) / 29.41 (Henry's Constant),

By including both the initial pH and pCO_2, the contribution of non-carbonic acids to soil acidity is accounted for in the difference between the pH predicted from pCO_2 alone and the actual pH of the soil solution. However, this equation does not take into account buffering by the soil particle surfaces, and therefore allows the solution pH to increase progressively as dissolution occurs, which in turn increases the calculated efficiency. As buffering in the soil tends to maintain the solution pH close to its initial value, we recommend that X not be calculated from the observed M, but rather a value of 10^{-10} mol kg^{-1}. As this value is several orders of magnitude below the H^+ concentration, it will have no meaningful effect on it and therefore gives X under constant pH. Though, in some cases, a detectable increase in pH with mineral application will occur, assuming that pH remains constant provides a conservative estimate of CO_2 uptake.

X*, a correction factor that assumes a constant pH, should therefore be derived as (see supplementary material for X* calculator):
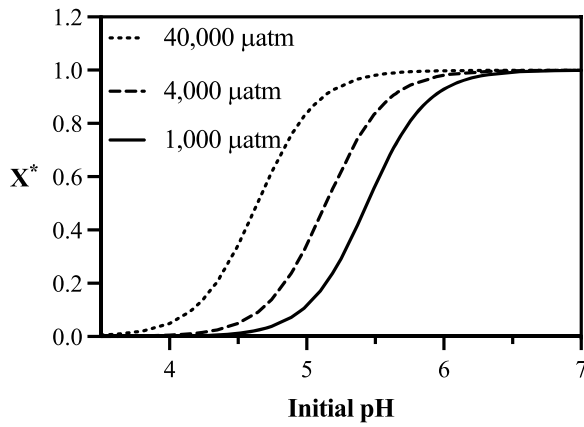
Fig. 1. Effect of soil gas CO_2 concentration on efficiency of CO_2 uptake, where $K_1 = 10^{-6.415}$ at 15 °C (Temperature has little effect between 5 and 25 °C: Fig. S1). 1000 µatm is the assumed minimum soil pCO_2, 4000 µatm represents 10 PAL (present atmospheric pCO_2), and 40,000 µatm represents 100 PAL.
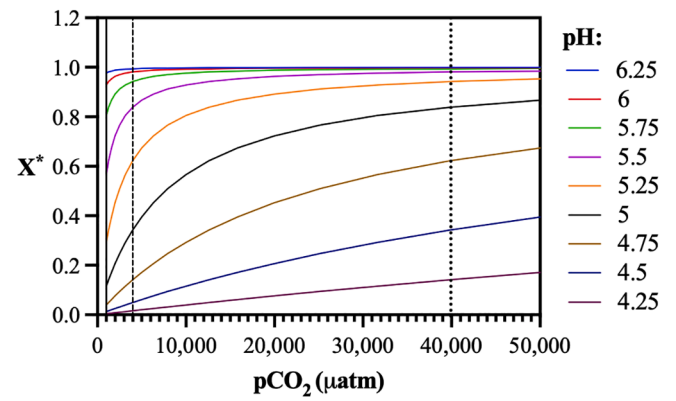

Fig. 2. Effect of pCO_2 on the efficiency (X^*) of CO_2 uptake. 1000 µatm (−) is the assumed minimum soil pCO_2, 4000 µatm (—) represents 10x atmospheric pCO_2, and 40,000 µatm (···) represents 100x atmospheric pCO_2.

can result in significant underestimation of CO_2 uptake (Fig. 2). The soil pCO_2 has the strongest effect on X^* around the pH range of 5 to 5.5. The effect of pCO_2 on X^* is weaker at higher pH's approaching pK_1 of the

$$X^* = \left\{ 10^{-20} - \left[\frac{10^{-10} \times K_1 \times [H_2CO_3]}{[H^+]} \right] - 10^{-10} \times [H^+] + \sqrt{ \left[\frac{10^{-10} \times K_1 \times [H_2CO_3]}{[H^+]} + 10^{-10} \times [H^+] - 10^{-20} \right]^2 + \frac{4 \times 10^{-30} \times K_1 \times [H_2CO_3]}{[H^+]} } \right\} \div 2 \times 10^{-20}$$

$$(8)$$

X^* can then be used to calculate the amount of CO_2 taken up on an area basis in kg ha^{-1} based on the difference in moles of positive charge associated with base cations per hectare between treatment (M_{treat}) and control ($M_{control}$) plots as follows:

$$\Delta\, CO_2\, \left(kg\ ha^{-1} \right) =\ X^* \times (M_{treat} - M_{control}) \times \frac{44.01\ g\ mol\ CO_2^{-1}}{1000} \qquad (9)$$

However, for a given pCO_2, there is a pH at which X^* has approached 1, and therefore there is no need to correct for dissolution by acids other than carbonic acid (Fig. 1).

Though it is often stated that soil gas pCO_2 ranges between 10 and 100 times present atmospheric pCO_2 (4000–40,000 µatm) (Lal, 2017), if pCO_2 is not known, we recommend conservatively assuming a pCO_2 of 1000 µatm. For the vast majority of the year, this is approximately the minimum soil pCO_2 that is reached in soil surface horizons (Albanito et al., 2009; Maier et al., 2010; Roland et al., 2015; Yonemura et al., 2009). Assuming this minimum pCO_2, the effect of stronger acids can be neglected for all soils with a pH above 6.29, as at this point X^* is calculated to be within 0.02 of maximum, which we consider to be sufficiently close to given that all other assumptions were made conservatively (Table 1). Given the considerable variability in soil pCO_2 both spatially and temporally (Albanito et al., 2009; Flechard et al., 2007; Maier et al., 2010), using this conservative estimate is likely much more practical than monitoring pCO_2.

However, it should be noted that making assumptions about pCO_2

carbonate system, and at lower pH's, in which X^* is controlled by the presence of stronger soil acids. Assuming that the soil CO_2 concentration is 1000 µatm does allow for a conservative estimate without having to measure CO_2 but can result in a significant reduction in the amount of carbon calculated to have been taken up and therefore potential carbon credits. For example, given a soil with a pH of 5.25 and a pCO_2 of 4000 µatm, which is often described as the lower end of soil CO_2 concentrations, assuming a pCO_2 of 1000 µatm would result in an underestimation of X^* by 0.33. Depending on the scale of the project and the pH of the soil, some pCO_2 monitoring therefore might be worthwhile in order to maximize potential income from carbon credits if the cost of monitoring is outweighed by the additional credits that could be gained by use of a more accurate value for pCO_2.

Identifying the minimum pH at which CO_2 uptake is sufficiently large to be worth the effort of applying for carbon credits also allows us to identify which farmland is worth applying silicate minerals to from a carbon uptake perspective. At the assumed pCO_2 (1000 µatm), any soils with a pH below 5.2 will have an X^* value of less than 0.25, likely implying that the amount of carbon credits possible may not be worth the cost of monitoring, or that monitoring of soil pCO_2 is necessary to identify if it is in fact high enough to allow for a sufficient increase in X^*.

As soil pH increases past 7.1, efficiency may be reduced due to the precipitation of carbonates (Kirk et al., 2015; Lal, 2017), which decreases CO_2 uptake by half (Eq. (10)).

$$Ca^{2+} + 2HCO_3^- -> CaCO_3 + CO_2 + H_2O \qquad (10)$$
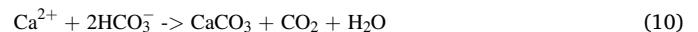
However, as the amount of precipitation expected can only be determined by a series of iterative calculations, it would be necessary to use PHREEQC or similar geochemical software to determine the extent of carbonate precipitation in a given soil (de Moel et al., 2013). Preferably, the increase in soil carbonates would be measured directly (Haque et al., 2020; Khalidy et al., 2021).

CO_2 uptake can therefore be measured based on changes in cation content without any correction for soil acids or measurement of

Table 1
Range of soil pH's over which excess acidity can be neglected. Lower limit based on $X^* > 0.98$.

pCO_2 (µatm)	Lower limit pH
40,000	5.49
4000	5.99
1000	6.29

carbonate precipitation only in soils in the narrow pH range of 6.29–7.1 (Table 1).

Soil buffering may temporarily neutralize the produced alkalinity if the released cations are exchanged with protons on the soil exchange complex, stabilizing the pH under which dissolution continues to take place (van Breemen et al., 1983). However, if these cations are leached out of the system, their release from the exchange complex, replacing H^+ in solution, will result in the reestablishment of the alkalinity initially created by the dissolution reaction. Depending on the residence time of water entering the system at the application site, it may remain in the groundwater for either a few weeks or thousands of years (Kessler and Harvey, 2001; Shiklomanov and Rodda, 2004). If eventually transported to the ocean, this dissolved inorganic carbon can remain stable in seawater between 100,000 and one million years as carbonate precipitation in the ocean is primarily due to biological activity and is otherwise inhibited in seawater (Renforth and Henderson, 2017). We have therefore not incorporated any assumed precipitation upon reaching the ocean into our calculations.

Cations taken up by plants are not included in our calculations of CO_2 uptake, as the exchange of protons for cations to maintain charge balance within the plant negates the initial production of alkalinity in the soil solution (Haynes, 1990). The re-release of these cations upon decomposition or burning of the harvested biomass, processes which consume protons (Binkley and Fisher, 2020), could still result in the production of alkalinity elsewhere (Banwart et al., 2009). However, the amount of CO_2 uptake at this later point would likewise be dependent on the carbonate chemistry of the solution in which this process occurs and the source of the hydrogen ion for the decomposition reaction. Any plant material or ashes thereof that is allowed to remain on the site will be exposed to the same conditions as the weathering minerals, and any cations released would simply be included in the site total and corrected accordingly. However, if this material is transported away from the site, the conditions and timescale under which it will later degrade are unknown and unlikely to be monitored, and therefore any CO_2 uptake associated with it is outside of the scope of carbon accounting due to this activity.

1.2. Glacial rock flour

Though most research on enhanced weathering has focused on the use of ground basalt or olivine due to their relatively fast weathering rates and high potential for CO_2 uptake (Amann et al., 2020, 2018; Amann and Hartmann, 2022; Dietzen et al., 2018; Garcia et al., 2019; Kelland et al., 2020; Lewis et al., 2021; Renforth et al., 2015; Rinder and von Hagke, 2021; Taylor et al., 2015; ten Berge et al., 2012; Vienne et al., 2022), energy intensive grinding is needed to reduce these materials to a useful grain size (<100μm) (Moosdorf et al., 2014). Glacial

rock flour (GRF) is found in nature with grain sizes much smaller than achievable by grinding on large scales- the median grain size of the Greenlandic GRF used in our study was only 2.6 μm, with a BET specific surface area of 19.6 $m^2 g^{-1}$. The small grain size and larger surface area of this material may compensate for being perhaps more chemically resistant to weathering than alternative silicate materials.

The CO_2 uptake capacity of a particular mineral is determined by the concentration of base cations, particularly those with a +2 charge (Mg^{2+}, Ca^{2+}). Mafic rocks like basalt and ultramafic rocks like dunite typically have a higher CO_2 uptake capacity than the felsic rocks that the glacial rock flour is primarily derived from. However, grain size sorting has resulted in the Ilulialik rock flour (Table 2: Ilulialik GRF) being depleted of larger quartz grains and enriched in biotite. The Ilulialik rock flour was collected from a marine deposit in the Nuuk fjord. Inputs to this deposit have first passed through Lake Tasersuaq, where more coarse-grained quartz sand (SiO_2) particles tend to settle from suspension, while more fine-grained micas that contain base cations would predominantly settle after flocculation in the marine delta (Sarkar, 2021). The composition and CO_2 uptake capacity of the GRF used in our study is therefore closer to the average composition and CO_2 uptake capacity of continental flood basalts than its source material due to the relative increase in the base cation content (Pearce et al., 1977). However, this GRF contains over three times more potassium than basalt, which may make it a more effective fertilizer. As a result of the marine depositional environment, the Ilulialik material also contains a small amount of NaCl (Sarkar, 2021) and minimal amounts of carbonate minerals (<1%).

The Ilulialik rock flour used in this experiment consists of 27.4% biotite, 18.6% oligoclase/andesine, 14.6% amphibole, 14.1% anorthite, 10.5% quartz, 4.3% Fe-oxide, 2.8% K-feldspar, and 2.4% muscovite (measured with ZEISS Sigma 300VP Field Emission Scanning Electron microscopy by the Geological Survey of Denmark and Greenland). Before being used in this field trial, this material was stored outdoors and exposed to rainfall, resulting in partial leaching of NaCl relative to the Ilulialik material described originally by Sarkar (2021).

2. Methods

In order to determine the effectiveness of glacial rock flour as an agricultural amendment intended to increase yield and take up CO_2 via enhanced weathering, glacial rock flour was applied to a certified organic farm near the town of Vojens in southern Denmark (55°12′16.4″N 9°15′55.9″E). The soils at the site are Cambic Arenosols formed on glacial outwash sands (GEUS, 2020), with a loamy sand texture, a pH_{H2O} of 5.8, and a pH_{CaCl2} of 5.0. These soils have a relatively low cation exchange capacity (7.16 meq 100 g^{-1}) and a soil organic matter content of 5.1%.

Table 2

Average composition of 3 types of GRF, continental flood basalts (Pearce et al., 1977), and average upper continental crust (Rudnick and Gao, 2003) in g 100 g^{-1}. * indicates the type of GRF used in this study (Ilulialik). R_{CO2}: Potential CO_2 uptake (ton CO_2 per ton of weathered rock) based on Mg^{2+}, Ca^{2+}, K^+, and Na^+ content (Renforth, 2012). Estimated Na^+ as NaCl (assuming all Cl^- is in the form of NaCl) was subtracted from the Ilulialik Na^+ content to calculate R_{CO2}. Chemical analysis of the GRF was performed by the center de Recherches Pétrographiques et Géochimiques (CRPG) at the French National center for Scientific Research (CNRS), Nancy, France (Carignan et al., 2001).

	Ilulialik GRF*	Tasersuaq GRF	Maalutu GRF	Continental Crust	Continental Flood Basalts
SiO_2	53.99	56.42	62.895	66.62	53.07
Al_2O_3	16.44	15.9005	15.6665	15.4	14.17
Fe_2O_3	8.55	6.765	5.1775	5.04	3.07
MnO	0.12	0.10125	0.0721	0.1	0.21
MgO	4.95	3.94	2.62	2.48	5.1
CaO	3.72	4.15	3.71	3.59	8.73
Na_2O	3.84	3.73	3.81	3.27	2.75
K_2O	3.50	2.84	2.86	2.8	1.14
TiO_2	0.71	0.59	0.49	0.64	2.06
P_2O_5	0.12	0.12	0.12	0.15	0.35
Cl (ppm)	4060	–	335	–	–
R_{CO2}	0.25	0.19	0.20	0.18	0.30

2.1. Experimental design and installation

Ilulialik GRF was applied at the site in 2019 at rates of 10 and 50 tons ha^{-1} (GRF$_{10}$ and GRF$_{50}$), and soil sampling was conducted over the following three years. The experimental design also included plots that had been amended with Patentkali®, a certified organic potash mineral fertilizer that was included as a reference K fertilization treatment for analysis of effects on yield (Gunnarsen et al., 2023). Plots were arranged in a randomized block design with four replicates (Fig. S2). Though differences in yield were analyzed in all treatment plots in Gunnarsen et al. (2023), here the plots that received Patentkali® are excluded from analysis.

GRF was weighed out and applied to 1 m^2 sections to ensure even application across the 3 × 20m treatment plots. The GRF was initially incorporated into the soil by harrowing to a depth of 80 mm in advance of furrowing. Before application of the GRF on April 17th, 2019, the entire area was fertilized with cow manure. The entire experimental field was fertilized with a biogas slurry before planting of potatoes in 2020, and with cow manure again before planting of spring wheat in 2021. In 2021 the spring wheat was also underseeded with a mix of clover, ryegrass, and festulolium (DSV Frøblanding Nr. 45) and fertilized with 2 kg ha^{-1} of manganese after planting. No further fertilizers or soil amendments were applied in any of the years (as mentioned above, this is a certified organic farm).

Potatoes were initially planted at the site in 2019, but due to their failure to germinate, the field was replanted with maize. Potatoes (Nofy variety) were successfully grown in 2020, and spring wheat was planted in 2021. Planting, harvest, and other relevant dates are outlined in Table S1. In 2020, the potatoes also received 125 mm of irrigation. The mean annual precipitation (2019–2021) for the region according to the Danish Meteorological Institute was 897mm and the mean annual temperature was 9.4 °C (DMI, 2019).

2.2. Sampling & analyses

Soil samples were taken multiple times each year. Though sampling procedures varied, when sampling depths were greater than 25 cm, measured values were normalized to a depth of 25 cm, either by sub-sampling and compositing samples from different depth intervals before chemical analysis or by using a weighted average of two analyzed depth intervals. The mean bulk density from the first set of samples (1.59 g cm^{-3}) was used to calculate exchangeable cations on an area basis (kg ha^{-1}) at all time points, with the exception of samples taken during the fall of the potato season (2020), which had unusually low bulk density in the 0–15 cm depth interval due to the creation of ridges. Here an equivalent soil mass approach was used rather than normalizing to a depth of 25 cm. Sampling dates and techniques are outlined in Table S2.

Soil samples were oven-dried at 50 °C, homogenized, and sieved to 2 mm. Ammonium acetate extractable Mg^{2+} and K$^+$ of all soil samples were determined according to Danish standard methods (Sørensen and Bülow-Olsen, 1994) which are typically used by commercial testing agencies in Denmark to determine soil exchangeable cations. However, ammonium nitrate, a more aggressive extractant (Abedin et al., 2012), has been shown to be better able to extract base cations than ammonium acetate (Borge, 1997). In order to determine if weathering and CO$_2$ uptake is better captured with an ammonium nitrate extraction, rather than the standard ammonium acetate extraction, samples from select time points that displayed the greatest differences from the control were re-analyzed using an ammonium nitrate extraction for comparison.

Three grams of soil were shaken overnight in 30ml of 1M NH$_4$NO$_3$, centrifuged for 10 min, and the supernatant retained. Ten ml of 1M NH$_4$NO$_3$ was then added to the soil, which was shaken for 10 min before centrifuging a second time. The supernatant was again retained, and the previous process was repeated once more. The collected supernatant was then vacuum-filtered through a 0.22 μm Millex-GP filter (Millipore) and the resulting solution was analyzed for exchangeable cations (Mg^{2+},

K$^+$, Ca^{2+}, Na$^+$) by ICP-MS on a PerkinElmer ELAN 6000.

Soil pH at all time points was measured in 0.01 M CaCl$_2$ at a soil-solution ratio of 1:2.5 (Sørensen and Bülow-Olsen, 1994) for the purpose of examining changes over time. The pH$_{H2O}$ of the initial samples from the control plots was measured at the same soil-solution ratio. This was used for calculating the CO$_2$ correction factor (X*) as pH$_{H2O}$ is more representative of the soil solution and therefore the conditions that the GRF is dissolving in than pH$_{CaCl2}$, which is typically lower as it includes protons displaced from the soil exchange complex (Flechard et al., 2007).

2.3. Statistical analysis

The effects of treatment and sampling time-point on measured response variables were tested using a linear mixed model ("nlme" in R version 4.1.0) fit to the data with treatment level and sampling point as interacting, categorical fixed factors and plot nested within block as a random factor to account for the experimental design and repeated measures over time (Pinheiro et al., 2017). Residual plots were inspected to ensure the model assumptions of normality and homogeneity of residuals were met. One control plot from Month 28 was removed from the pH analysis as an outlier as it was unrealistically high. To account for heteroskedasticity, the "weights" function was used to allow variances to differ between sampling points. Treatment level was also included in the weights function when it improved the AIC of the model. Means of treated plots were compared to the control at each time point by use of Dunnett's test (α=0.05) ("emmeans" in R). Differences in the mean pH across all treatments and ammonium acetate extractable Mg^{2+} (Mg$_{AA}$) of the control plots between consecutive seasons were also tested ("consec" in "emmeans", "mvt" correction used for multiple comparisons). A linear model was used to test the relationship between Mg$_{AA}$ and ammonium nitrate extractable Mg^{2+} (Mg$_{AN}$) using all samples from the three months in which both types of extraction were performed.

3. Results

In September 2019, five months after the GRF application (Month 5), there was an increase of Mg$_{AA}$ in the GRF$_{50}$ plots of 52 kg ha^{-1} ($p = $ .010), from 172±9 kg ha^{-1} in the control plots to 225±16 kg ha^{-1} in the GRF$_{50}$ plots (Fig. 3). By November (Month 7), the difference had decreased to 31 kg ha^{-1} ($p = $ .002), and by the following spring (Month 12), the difference between GRF$_{50}$ and the control was minimal and no longer significant. A significant increase in Mg$_{AA}$ was observed again in July of 2021 (Month 28), at which point GRF$_{50}$ increased Mg$_{AA}$ by 37 kg
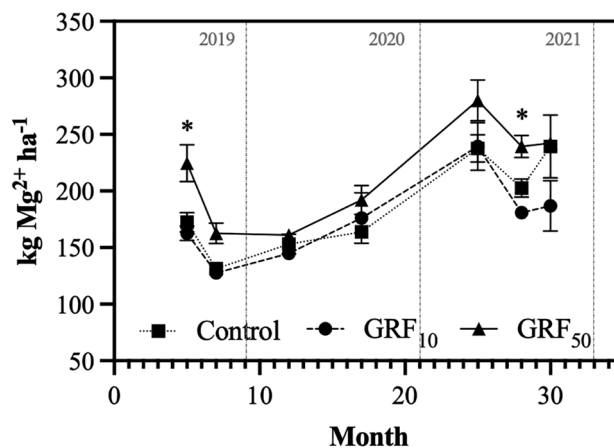

Fig. 3. Ammonium acetate extractable Mg^{2+} treatment means (kg Mg^{2+} ha^{-1} to 30 cm depth) over time (months after GRF application). GRF$_{10}$ indicates the 10 t GRF ha^{-1} treatment and GRF$_{50}$ indicates 50 t GRF ha^{-1}. Error bars are SE. * indicates GRF$_{50}$ is significantly greater than the control ($p < $ .05).
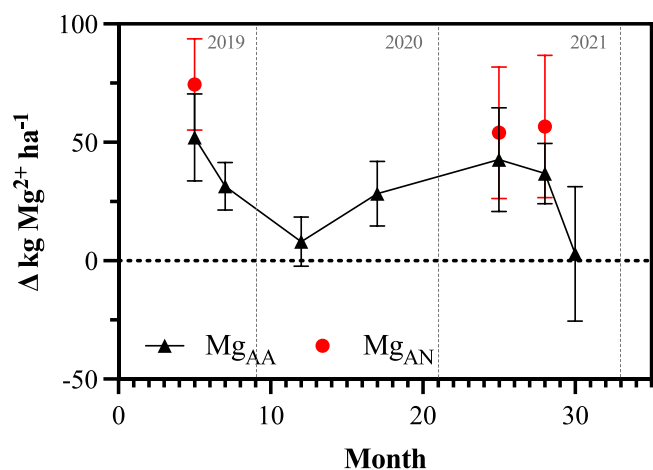
Fig. 4. Difference in ammonium acetate extractable Mg^{2+} (Mg_{AA}) between the GRF_{50} (50 t GRF ha^{-1}) and control plots over time and, at three time points, the difference in ammonium nitrate extractable Mg^{2+} (Mg_{AN}) between the GRF_{50} and control plots. Error bars are SE.
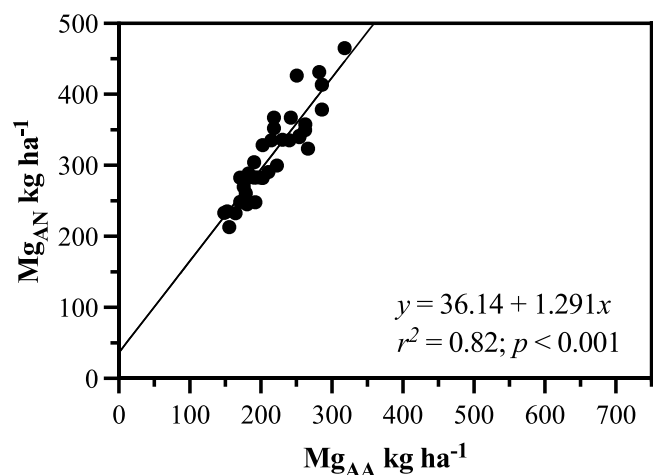

Fig. 5. Correlation between ammonium acetate extractable Mg^{2+} (Mg_{AA}) and ammonium nitrate extractable Mg^{2+} (Mg_{AN}).

ha^{-1} (from 203±16 to 239±10) ($p = .010$). At no point in time was the GRF_{10} treatment significantly different from the control.

Soil samples from Months 5, 25, and 28, which showed the greatest differences in Mg_{AA} between the control and GRF_{50} plots, were also subjected to an ammonium nitrate extraction (Fig. 4). Though there was a trend towards elevated Mg_{AN} in all months tested, this was only significant in Month 5, in which Mg_{AN} was 74.4 kg ha^{-1} greater in the GRF_{50} plots than the control plots ($p = .016$) (Fig. 4). Even though the difference in Mg_{AN} between the control and GRF_{50} in Month 28 (56.7 kg ha^{-1}) was greater than the significant difference in that month in Mg_{AA} (36.77 kg ha^{-1}, $p = .010$), it was statistically insignificant ($p = .190$). This may be due to the much higher variability around the mean observed in the GRF_{50} Mg_{AN} values in this month. A significant linear correlation was found between Mg_{AA} and Mg_{AN} ($p < .001$), showing that ammonium nitrate consistently extracted more exchangeable Mg^{2+} than ammonium acetate (Fig. 5).

Na_{AN} was elevated above the control in the GRF_{50} plots in the first month sampled (Month 5) ($p < .001$), having increased Na_{AN} by 233 kg ha^{-1} from 92±7 kg ha^{-1} in the control plots to 325±7 kg ha^{-1} in the GRF_{50} plots in that month. There was no significant increase with treatment in Month 25, though this difference was apparent again in Month 28, but the increase was much smaller 17.6 kg ha^{-1} ($p = .008$).

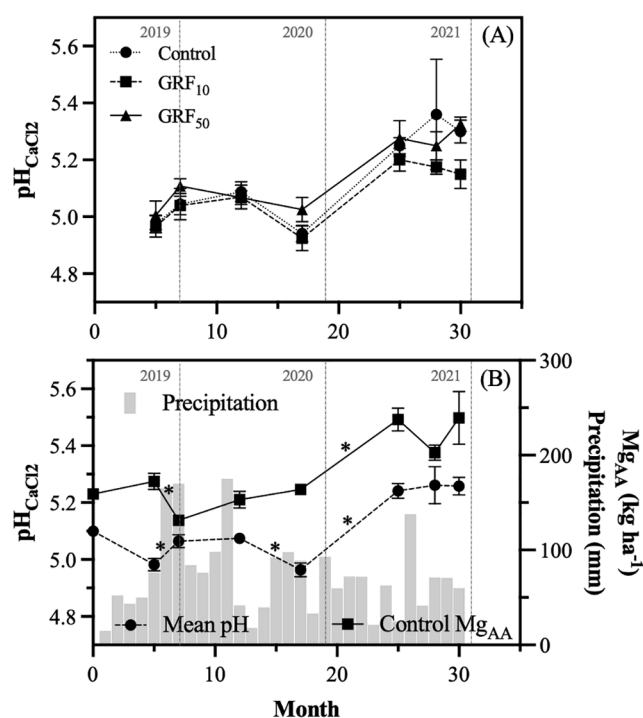**Fig. 6.** A) pH_{CaCl2} of each treatment [Control, GRF_{10} (10 t GRF ha^{-1}), and GRF_{50} (50 t GRF ha^{-1})] over time. Error bars are SE. B) Mean pH_{CaCl2} across all plots and ammonium acetate extractable Mg^{2+} (Mg_{AA}; kg ha^{-1}) in the control plots over time. Point 0 represents pretreatment soil measurements of the field. * Indicates significant difference between consecutive values. Error bars are SE. Gray bars indicate monthly precipitation (mm).

Though the trend was towards higher K_{AN} with GRF_{50}, this increase was only significant in Month 28 ($p = .019$). Treatment had no effect on K_{AA} or Ca_{AN} any point.

There were no significant differences in pH with treatment (Fig. 6A), though there were significant differences in pH over time. A large increase in soil pH and Mg_{AA} after the harvest of potatoes in 2020 must be noted (Fig. 6B). Between Months 17 and 25 pH increased by 0.28 points ($p < .001$), and Mg_{AA} in the control plots increased by 74 kg ha^{-1} ($p < .001$). We suspect that the significant disturbance of the soil during the process of harvesting potatoes likely induced additional organic matter decomposition, releasing nutrients to the soil and increasing pH (Feng and Balkcom, 2017).

3.1. Calculation of CO_2 uptake

Our calculations of CO_2 uptake at Vojens are based upon differences in Mg_{AN} with treatment. Though the release of any base cations from GRF dissolution could result in the uptake of CO_2, Mg^{2+} plays a larger role than the other cations. Due to its relatively high concentration, its +2 charge, and its lower ratio of mass to charge compared to Ca^{2+}, Mg^{2+} accounts for 44% of potential CO_2 uptake by the dissolution of GRF. Mg^{2+} is also less likely to be taken up as a plant nutrient than K^+, meaning the creation of alkalinity associated with its release is less likely to be negated.

With the exception of Na^+, Mg^{2+} was also the only soil exchangeable cation that significantly increased with the application of GRF at Vojens, and therefore it is the only cation that we can confidently base our calculations of CO_2 uptake on. We did not include Na^+, even though significant, as it is unknown what portion of the Na^+ released is sourced from the GRF itself and not the small amount of the highly soluble NaCl that accompanies it. NaCl comprises approximately 9% of the Na^+ contained in the Ilulialik material, but its dissolution does not result in the uptake of CO_2. Differences in soil Mg^{2+} are also likely to be more

easily detectable than differences in soil Ca^{2+}, as most soils contain significantly greater and correspondingly more variable amounts of exchangeable Ca^{2+} than Mg^{2+}. In the initial sampling of the control plots, the standard deviation of Mg_{AN} was 8 kg ha^{-1}, whereas the standard deviation of Ca_{AN} was 238 kg ha^{-1}, making it difficult to detect increases in Ca_{AN} resulting from silicate mineral application due to the inherently large background variability.

The total kg Mg^{2+} ha^{-1} released from weathering at the higher application rate was calculated by adding the difference in Mg_{AN} between the control and GRF$_{50}$ in Month 5 and the difference between the control and GRF$_{50}$ in Month 28, the two peaks, minus the difference that remained in the spring of 2020 (Month 12) converted from Mg_{AA} to Mg_{AN} according to the linear regression of the relationship between these values (Fig. 5). Accordingly, we determined that a total of 120.7 kg Mg^{2+} ha^{-1} was released by the weathering of GRF. Given that a total of 1525 kg ha^{-1} of Mg^{2+} was applied with the GRF, this equates to an Mg^{2+} release rate of 7.9% over the 3 growing seasons. Though a significant increase in plant uptake of Mg^{2+} with treatment was detected in Gunnarsen et al. (2023), differences in plant Mg^{2+} were not included when calculating weathering rates as they were several orders of magnitude lower than differences in soil available Mg^{2+} and therefore negligible.

Based on differences in soil available Mg^{2+} without correction for stronger acids, CO_2 uptake would have been calculated to be 437 kg ha^{-1}. Given the mean pH_{H2O} of the control plots in 2019 (5.79) and an assumed pCO_2 of 1000 µatm, the value of X* at Vojens is calculated to be 0.83. Accounting for stronger acids, a minimum of 364 kg CO_2 ha^{-1} was taken up over this course of the study, indicating that uptake without this correction would have been overestimated by up to 20%. These values are dependent on our assumptions about soil pCO_2 at the site. If pCO_2 were in fact 4000 µatm, a level often stated to be the lower end of soil pCO_2 values (Lal, 2017), instead of the assumed 1000 µatm, X* would be 0.12 higher: 0.95. If pCO_2 were known to be 10,000 µatm or greater, the pH of the soil at Vojens is sufficiently high that a correction for stronger acids would not be necessary.

If we assume that Ca^{2+} and Na^+ were both released and leached at the same rate as Mg^{2+}, but differences were masked by the large inherent soil background variation and concurrent dissolution of NaCl, respectively- and include a proportionally equivalent amount of Ca^{2+} and Na^+ weathering, the estimated CO_2 uptake for GRF$_{50}$ increases to 728 kg CO_2 ha^{-1}, or 14.6 kg CO_2 per ton of GRF over 3 years. This calculation only includes Na^+ that was not present as NaCl, assuming that all Cl was in the form of NaCl. K^+ is not included as seemed to be completely taken up by plant growth (Gunnarsen et al., in review), though a difference in K_{AN} was observed with treatment in the last month measured, which was sampled after harvest when there was no longer any plant uptake.

Table 3

Comparison of CO_2 uptake due to glacial rock flour application with previous estimates of CO_2 uptake due to application of ground basalt. A: (Lewis et al., 2021); B: (Gudbrandsson et al., 2011); C: (Navarre-Sitchler and Brantley, 2007); *approximate- read from graph.

	This study	Kelland et al. (2020)	Rinder and von Hagke (2021)
Material	Ilulialik GRF	Basalt	Basalt
Grain Size (µm)	D50= 2.6	D80 = 1250	<10
Application Rate (t ha^{-1})	50	100	N/A- Shrinking core model
BET surface area m^2 g^{-1}	19.6	7.35	18.61
Soil pH	5.79	6.6	5.84[B]
BET normalized Mg^{2+} elemental release rate (mol Mg^{2+} m^{-2} s^{-1})	$10^{-12.62}$	$10^{-12.18}$	$10^{-12.45 \ B}$
% Mg^{2+}	2.98	1.3[A]	1.29[C]
CO_2 uptake (kg CO_2 t^{-1} over 3 years)	14.6	~27	~80*

4. Discussion

The observed dissolution rates of Ilulialik GRF, though consistently lower, are on the same order of magnitude as basalt. Steady state laboratory dissolution rates of Ilulialik GRF were found to be around $10^{-10.5}$ mol Si m^{-2} s^{-1} (Sarkar, 2021), while the dissolution rate of crystalline basalt tends to be greater than 10^{-10} mol Si m^{-2} s^{-1} at comparable experimental conditions (Gudbrandsson et al., 2011). Likewise, the observed BET normalized Mg^{2+} elemental release rate of Ilulialik GRF$_{50}$ ($10^{-12.62}$ mol Mg^{2+} m^{-2} s^{-1}) at Vojens is approximately 30–60% lower than the range of observed and modelled rates of Mg^{2+} release from basalts added to soils ($10^{-12.18}$ and $10^{-12.45}$ mol Mg^{2+} m^{-2} s^{-1}, respectively) (Kelland et al., 2020; Rinder and von Hagke, 2021), despite the fact that these basalts contain less Mg^{2+} than the GRF (Table 3).

Based on these release rates and reactive transport modeling, Kelland et al. (2020) predicted approximately 27 kg CO_2 uptake per ton of basalt in columns treated with 100 t ha^{-1} of basalt with a D80 grain size of 1250 µm over 3 years. This is almost twice as much as the 14.6 kg CO_2 uptake per ton of GRF observed over 3 years at our site. Rinder and Von Hagke (2021) predicted even greater rates of CO_2 uptake per ton of basalt. Using a shrinking core model of basalt with a grain size of <10 µm, they predict approximately 80 kg CO_2 uptake per ton of basalt after 3 years. This amount of CO_2 uptake is much greater than that observed by this study or Kelland et al. (2020) in the field, but the authors do note that the weathering rate used in their model may be on the high end as it was determined under laboratory conditions and at a higher temperature than expected in the field (Gudbrandsson et al., 2011; Rinder and von Hagke, 2021). The effect of application rate is also not accounted for in this model. It appears that CO_2 uptake associated with the application of GRF may not be as high as that of basalt, but given the wide variety of grain sizes, application rates, and environments studied, research conducted under more uniform conditions for better comparison is needed before this can be known for certain.

Our calculations of CO_2 uptake at Vojens are based on the assumption that the difference in soil Mg^{2+} with treatment disappeared over the course of the winter rainy season due to leaching and not precipitation of secondary minerals. This assumption is fairly reasonable given that the sandy soils at this site are well drained with a low CEC. These properties, combined with higher leaching rates in the autumn and winter when the lack of crop cover combined with surplus rainfall result in a positive water balance (Jabloun et al., 2015), render it likely that cations would be transported out of the soil before secondary minerals could form. Leaching of Mg^{2+} as high as 69.2 kg Mg^{2+} ha^{-1} has been observed at other sites (Mesic et al., 2007), which suggests that it is possible that 64 kg Mg^{2+} ha^{-1}, the observed decrease in difference between GRF$_{50}$ and the control between harvest and spring measurements after the first growing season, could have been leached away over the winter months. The export of Mg^{2+} from the system prevents the reversal of alkalinity production in later seasons by plant uptake of Mg^{2+} in exchange for H^+, unless plant uptake occurs in depths deeper than those sampled (>25cm). This is unlikely with potatoes, which primarily root in the plow layer, but could be possible under maize, which has a much deeper root system (Yamaguchi and Tanaka, 1990). However, as plant demand for Mg^{2+} is relatively low, and plant uptake was observed to be several orders of magnitude lower than the amount accumulated in the soil, later uptake may only have a negligible on CO_2 uptake.

Further research is needed to investigate the effects of different crop types on GRF dissolution and the associated CO_2 uptake. Cereals, including maize, are known to be more efficient at taking up non-exchangeable K^+ than potatoes due to differences in their root systems (Wang et al., 2000; White, 2013), which may have resulted in reduced weathering under the potato crop. The possibly lower weathering ability of potatoes may also be the reason why no significant difference was detected in Mg_{AA} in the second year, unlike the first and third.

Our findings recommend the use of ammonium nitrate extractions

over ammonium acetate for acidic soils to ensure that increases in exchangeable cations and consequently CO_2 uptake are not underestimated. However, additional research is still needed to improve recommendations for the measurement of necessary parameters- such as timing and frequency of measurements of pH, exchangeable cations, and pCO_2 for a variety of cropping systems and environments. As farmers are unlikely to have a suitable control field for comparison with the treated field to determine the increase in Mg^{2+} with treatment, alternative methods of detecting the release of cations will be necessary. This could potentially be done by establishing site-specific baselines in absence of a control, which will likely require monitoring of a site for at least a year in advance of treatment in order to identify seasonal variations in soil pH and nutrient content. Based on this, farmers can select time points for sampling that are reflective of leaching patterns at their particular site.

For example, at Vojens, sampling could be done in the spring, after the majority of over-winter leaching has occurred and again after harvest but before the rainy season starts again and leaching recommences, when weathering products have had an opportunity to build up in the soil. By comparing these two time points, as long as no other amendments were added to the field, any increase in Mg^{2+} can be assumed to be due to the dissolution of the silicate minerals. The data from Vojens supports the use of this method, as the difference in Mg_{AA} between GRF_{50} and the control in the fall of 2020 (Month 17) (28.3 kg ha^{-1}) is fairly comparable to the difference (31.1 kg ha^{-1}) in the Mg_{AA} of GRF_{50} between the spring of 2020 (Month 12) and the fall. This would, however, be complicated by the addition of any other Mg^{2+}-bearing soil amendments, or if significant soil disturbance results in increased organic matter decomposition and nutrient release (Feng and Balkcom, 2017), such as observed after mechanized potato harvesting at Vojens. Additional research is needed to determine how to best account for such effects in absence of a control.

Though silicate mineral treatments can increase soil pH (Dietzen et al., 2018), the use of a constant pH for the efficiency calculations is still preferred as these differences, in many cases, will be smaller than or comparable to seasonal differences in pH (Wuest, 2015). This was the case at Vojens, where sampling point had a significant effect on soil pH but treatment did not. Because of this, pre-treatment soil monitoring is also needed to learn what time of year soil pH tends to be lowest at a site. Soil pH for CO_2 uptake calculations should be measured in water at this lowest point in order to ensure a conservative estimate of CO_2 consumed. However, large changes in pH, such as those observed after potato harvesting, may be reason to change the pH used in later calculations of the efficiency of CO_2 uptake.

Further research is needed to confirm the effectiveness of the proposed correction. This could be done by collecting leachate and comparing CO_2 uptake predicted from changes in soil cations with measured alkalinity fluxes. Experimental measurement of exchangeable cations in leachate as a proxy for CO_2 uptake via weathering should also be corrected according to the proposed methods and could also be used to ground truth estimates derived from soil samples. Taylor et al. (2021) reported that the modeled stream-water bicarbonate flux at Hubbard Brook after wollastonite application to the watershed was generally 20% lower than would have been calculated by the Ca^{2+} flux. This correlates exceedingly well with the mean X* of 0.21 calculated from the pH and DIC (pCO_2 calculated using CO2SYS v2.1 (Pierrot et al., 2006)) of all soil solution samples collected in the B horizon since the application of wollastonite to the site (Driscoll, 2022).

The function described in this paper allows for an estimate of the CO_2 uptake efficiency of a site in advance of mineral applications, which will allow for improved site selection if the goal of application is strictly CO_2 uptake or cost savings on monitoring if minerals are applied to improve plant growth but unlikely sequester sufficient carbon. However, there may still be a climate benefit to applying silicate minerals even in the case of low pH, as the neutralization of this acidity is usually done with agricultural lime ($CaCO_3$). The dissolution of lime releases CO_2, so the use of silicate minerals as an alternative amendment for to increase soil pH can prevent one source of agricultural CO_2 emissions (Dietzen et al., 2018).

5. Conclusion

Here we demonstrated the application of a protocol for CO_2 uptake calculations due to enhanced weathering that accounts for dissolution of silicate minerals by other soil inorganic acids in addition to H_2CO_3. In doing so, we have also shown that the application of Greenlandic glacial rock flour to an acidic agricultural field can take up approximately 14.6 kg CO_2 per ton of GRF over 3 years at an application rate of 50 t ha^{-1}, totaling 728 kg CO_2 ha^{-1}. Our estimated CO_2 uptake does not take into account emissions due to extraction, transportation, and application (Wulffeld, 2021), which can delay the net positive effect of silicate mineral applications (Rinder and von Hagke, 2021). These would need to be thoroughly accounted for before mineral application to ensure that it is possible for the uptake due to weathering to outweigh emissions due to transportation within a reasonable time frame. However, as the transportation sector is progressively de-carbonized (Sims et al., 2014), the reductions in net uptake due to transportation will become less of a hindrance to the effectiveness of this method of carbon removal. Further research is needed to ground truth our proposed method of calculating CO_2 uptake and to determine best practices for soil cation sampling across a range of environmental conditions in order to provide farmers with clear protocols for monitoring and verifying CO_2 uptake associated with enhanced mineral weathering.

Authors' contributions

Conceptualization, C.D., M.T.R.; Methodology, C.D.; Formal analysis, C.D.; Investigation, C.D.; Writing – original draft, C.D. Writing – review & editing, C.D. and M.T.R. Funding acquisition, M.T.R.; Supervision, M.T.R.

CRediT authorship contribution statement

Christiana Dietzen: Conceptualization, Methodology, Formal analysis, Investigation, Writing – original draft, Writing – review & editing. **Minik T. Rosing:** Conceptualization, Writing – review & editing, Funding acquisition, Supervision.

Declaration of Competing Interest

The authors declare that they have no known competing financial interests or personal relationships that could have appeared to influence the work reported in this paper.

Data availability

https://doi.org/10.17894/ucph.16fbf798–6de6–40d6–8437-e70cd0a42fc1

Acknowledgements

Supplementary materials

Supplementary material associated with this article can be found in the online version, at doi:10.1016/j.ijggc.2023.103872.

References

Abedin, J., Beckett, P., Spiers, G., 2012. An evaluation of extractants for assessment of metal phytoavailability to guide reclamation practices in acidic soilscapes in northern regions. Can. J. Soil Sci. 92, 253–268. https://doi.org/10.4141/CJSS2010-061.

Albanito, F., Saunders, M., Jones, M.B., 2009. Automated diffusion chambers to monitor diurnal and seasonal dynamics of the soil CO2 concentration profile. Eur. J. Soil Sci. 60, 507–514. https://doi.org/10.1111/j.1365-2389.2009.01154.x.

Amann, T., Hartmann, J., 2019. Ideas and perspectives : synergies from co-deployment of negative emission technologies. Biogeosciences 16, 2949–2960. https://doi.org/10.5194/bg-16-2949-2019.

Amann, T., Hartmann, J., 2022. Carbon accounting for enhanced weathering. Front. Clim. 4, 849948 https://doi.org/10.3389/fclim.2022.849948.

Amann, T., Hartmann, J., Struyf, E., de Oliveira Garcia, W., Fischer, E.K., Janssens, I., Meire, P., Schoelynck, J., 2018. Constraints on Enhanced Weathering and related carbon sequestration – a cropland mesocosm approach. Biogeosci. Discuss. 1–21. https://doi.org/10.5194/bg-2018-398.

Amann, T., Hartmann, J., Struyf, E., De Oliveira Garcia, W., Fischer, E.K., Janssens, I., Meire, P., Schoelynck, J., Garcia, W.D.O., Fischer, E.K., Janssens, I., 2020. Enhanced Weathering and related element fluxes – a cropland mesocosm approach. Biogeosciences 17, 103–119. https://doi.org/10.5194/bg-17-103-2020.

Banwart, S.A., Berg, A., Beerling, D.J., 2009. Process-based modeling of silicate mineral weathering responses to increasing atmospheric CO2 and climate change. Glob. Biogeochem. Cycles 23, 1–13. https://doi.org/10.1029/2008GB003243.

Beerling, D.J., Leake, J.R., Long, S.P., Scholes, J.D., Ton, J., Nelson, P.N., Bird, M., Kantzas, E., Taylor, L.L., Sarkar, B., Kelland, M., DeLucia, E., Kantola, I., Müller, C., Rau, G., Hansen, J., 2018. Farming with crops and rocks to address global climate, food and soil security. Nat. Plants 4. https://doi.org/10.1038/s41477-018-0108-y.

Binkley, D., Fisher, R.F., 2020. Ecology and management of forest soils: fourth edition, ecology and management of forest soils: fifth edition. 10.1002/9781118422342.

Borge, A., 1997. A comparison of buffered and unbuffered ammonium salts to determine exchangeable base cations in acid soils. Commun. Soil Sci. Plant Anal. 28, 1421–1428. https://doi.org/10.1080/00103629709369884.

Carignan, J., Hild, P., Mevelle, G., Morel, J., Yeghicheyan, D., 2001. Routine analyses of trace elements in geological samples using flow injection and low pressure on-line liquid chromatography coupled to ICP-MS: a study of geochemical reference materials BR, DR-N, UB-N, AN-G and GH. Geostandards Geoanal. Res. 25, 187–198. https://doi.org/10.1111/j.1751-908X.2001.tb00595.x.

de Moel, P.J., van der Helm, A.W.C., van Rijn, M., van Dijk, J.C., van der Meer, W.G.J., 2013. Assessment of calculation methods for calcium carbonate saturation in drinking water for DIN 38404-10 compliance. Drinking Water Eng. Sci. 6, 115–124. https://doi.org/10.5194/dwes-6-115-2013.

Dietzen, C., Harrison, R., Michelsen-Correa, S., 2018. Effectiveness of enhanced mineral weathering as a carbon sequestration tool and alternative to agricultural lime : an incubation experiment. Int. J. Greenhouse Gas Control 74, 251–258. https://doi.org/10.1016/j.ijggc.2018.05.007.

DMI, 2019. Vejrarkiv [WWW Document]. Vejrarkiv (Weather Archive): Haderslev. URL http://www.dmi.dk/vejrarkiv/(accessed 11.3.22).

Driscoll, C.T., 2022. Chemistry of freely-draining soil solutions at the Hubbard Brook Experimental Forest, Watershed 1, 1996 - present ver 11. Environmental Data Initiative. 10.6073/pasta/90b588b9a04bfeefa29024929b0af1f4.

Feng, Y., Balkcom, K.S., 2017. Nutrient cycling and soil biology in row crop systems under intensive tillage, in: soil health and intensification of agroecosystems. Elsevier Inc. 231–255. https://doi.org/10.1016/B978-0-12-805317-1.00011-7.

Flechard, C.R., Neftel, A., Jocher, M., Ammann, C., Leifeld, J., Fuhrer, J., 2007. Temporal changes in soil pore space CO2 concentration and storage under permanent grassland. Agric. For. Meteorol. 142, 66–84. https://doi.org/10.1016/j.agrformet.2006.11.006.

Garcia, W.D.O., Amann, T., Hartmann, J., Karstens, K., Popp, A., Boysen, L.R., Smith, P., Goll, D., De Oliveira Garcia, W., Amann, T., Hartmann, J., Karstens, K., Popp, A., Boysen, L.R., Smith, P., Goll, D., de Oliveira Garcia, W., Amann, T., Hartmann, J., Karstens, K., Popp, A., Boysen, L.R., Smith, P., Goll, D., 2019. Impacts of Enhanced Weathering on biomass production for negative emission technologies and soil hydrology. Biogeosci. Discuss. 17, 1–35. https://doi.org/10.5194/bg-2019-386.

GEUS, 2020. Surface Geology Map of Denmark 1:25.000 [WWW Document]. URL https://eng.geus.dk/products-services-facilities/data-and-maps/maps-of-denmark (accessed 11.3.22).

Gudbrandsson, S., Wolff-boenisch, D., Gislason, S.R., Oelkers, E.H., 2011. An experimental study of crystalline basalt dissolution from 2<pH<11 and temperatures from 5 to 75°C. Geochim. Cosmochim. Acta 75, 5496–5509. https://doi.org/10.1016/j.gca.2011.06.035.

Gunnarsen, K.C., Jensen, L.S., Rosing, M.T., Dietzen, C., 2023. Greenlandic glacial rock flour improves crop yield in organic agricultural production. Nutrient Cycling in Agroecosystems. In Press.

Haque, F., Santos, R.M., Chiang, Y.W., 2020. Optimizing inorganic carbon sequestration and crop yield with wollastonite soil amendment in a microplot study. Front. Plant Sci. 11 https://doi.org/10.3389/fpls.2020.01012.

Haque, F., Santos, R.M., Dutta, A., Thimmanagari, M., Chiang, Y.W., 2019. Co-benefits of wollastonite weathering in agriculture: CO2 sequestration and promoted plant growth. ACS Omega 4, 1425–1433. https://doi.org/10.1021/acsomega.8b02477.

Harley, A.D., Gilkes, R.J., 2000. Factors influencing the release of plant nutrient elements from silicate rock powders : a geochemical overview. Nutr. Cycling Agroecosystems 56, 11–36. https://doi.org/10.1023/A:1009859309453.

Hartmann, J., West, A.J., Renforth, P., Köhler, P., De La Rocha, C.L., Wolf-gladrow, D.A., Dürr, H.H., Scheffran, J., Rocha, C.L.D.L., Wolf-gladrow, D.A., Dürr, H.H., Scheffran, J., De La Rocha, C.L., Wolf-gladrow, D.A., Scheffran, J., 2013. Enhanced chemical weathering as a geoengineering strategy to reduce atmospheric carbon dioxide, supply nutrients, and mitigate ocean acidification. Rev. Geophys. 51, 113–149. https://doi.org/10.1002/rog.20004.

Haynes, R.J.J., 1990. Active ion uptake and maintenance of cation-anion balance : a critical examination of their role in regulating rhizosphere pH. Plant Soil 126, 247–264.

IPCC, 2018. Summary for Policymakers. In: Global Warming of 1.5°C. An IPCC Special Report On the Impacts of Global Warming of 1.5°C Above Pre-Industrial Levels and Related Global Greenhouse Gas Emission pathways, in the Context of Strengthening the Global Response to.

Jabloun, M., Schelde, K., Tao, F., Olesen, J.E., 2015. Effect of temperature and precipitation on nitrate leaching from organic cereal cropping systems in Denmark. Eur. J. Agronomy 62, 55–64. https://doi.org/10.1016/j.eja.2014.09.007.

Kelland, M.E., Wade, P.W., Lewis, A.L., Taylor, L.L., Sarkar, B., Andrews, M.G., Lomas, M.R., Cotton, T.E.A.E.A., Kemp, S.J., James, R.H., Pearce, C.R., Hartley, S.E., Hodson, M.E., Leake, J.R., Banwart, S.A., Beerling, D.J., Wade, P.W., Johnson, D.A., Lewis, A.L., Andrews, M.G., Lomas, M.R., Cotton, T.E.A.E.A., Kemp, S.J., Taylor, L.L., James, R.H., Pearce, C.R., Hartley, S.E., Hodson, M.E., Leake, J.R., Banwart, S.A., Beerling, D.J., Sarkar, B., Andrews, M.G., Lomas, M.R., Cotton, T.E.A.E.A., Kemp, S. J., James, R.H., Pearce, C.R., Hartley, S.E., Hodson, M.E., Leake, J.R., Banwart, S.A., Beerling, D.J., 2020. Increased yield and CO2 sequestration potential with the C4 cereal Sorghum bicolor cultivated in basaltic rock dust-amended agricultural soil. Glob. Chang. Biol. 26, 3658–3676. https://doi.org/10.1111/gcb.15089.

Kessler, T.J., Harvey, C.F., 2001. The global flux of carbon dioxide into groundwater. Geophys. Res. Lett. 28, 279–282. https://doi.org/10.1029/2000GL011505.

Khalidy, R., Haque, F., Chiang, Y.W., Santos, R.M., 2021. Monitoring pedogenic inorganic carbon accumulation due to weathering of amended silicate minerals in agricultural soils. JoVE 2021. https://doi.org/10.3791/61996.

Kirk, G.J.D.D., Versteegen, A., Ritz, K., Milodowski, A.E., 2015. A simple reactive-transport model of calcite precipitation in soils and other porous media. Geochim. Cosmochim. Acta 165, 108–122. https://doi.org/10.1016/j.gca.2015.05.017.

Lal, R. (Ed.), 2017. Encyclopedia of Soil Science, 3rd ed. CRC Press; Taylor & Francis Group, LLC.

Lewis, A.L., Sarkar, B., Wade, P., Kemp, S.J., Hodson, M.E., Loong Yeong, K., Davies, K., Nelson, P.N., Bird, M.I., Masters, M.D., DeLucia, E., Leake, J.R., Banwart, S.A., Beerling, D.J., Taylor, L.L., Yeong, K.L., Davies, K., Nelson, P.N., Bird, M.I., Kantola, I.B., Masters, M.D., DeLucia, E., Leake, J.R., Banwart, S.A., Beerling, D.J., 2021. Effects of mineralogy, chemistry and physical properties of basalts on carbon capture potential and plant-nutrient element release via enhanced weathering. Appl. Geochem. 132, 105023 https://doi.org/10.1016/j.apgeochem.2021.105023.

Maier, M., Schack-Kirchner, H., Hildebrand, E.E., Holst, J., 2010. Pore-space CO2 dynamics in a deep, well-aerated soil. Eur. J. Soil Sci. 61, 877–887. https://doi.org/10.1111/j.1365-2389.2010.01287.x.

Mesic, M., Kisić, I., Bašić, F., Butorac, A., Zgorelec, Ž., Cašpar, I., 2007. Losses of Ca, Mg and SO4 2-S with drainage water at fertilisation with different nitrogen rates. Agriculturae Conspectus Scientificus 72, 53–58.

Moosdorf, N., Renforth, P., Hartmann, J., 2014. Carbon dioxide efficiency of terrestrial enhanced weathering. Environ. Sci. Technol. 48, 4809–4816. https://doi.org/10.1021/es4052022.

Navarre-Sitchler, A., Brantley, S., 2007. Basalt weathering across scales. Earth Planet. Sci. Lett. 261, 321–334. https://doi.org/10.1016/j.epsl.2007.07.010.

Pearce, T.H., Gorman, B.E., Birkett, T.C., 1977. The relationship between major element chemistry and tectonic environment of basic and intermediate volcanic rocks. Earth Planet. Sci. Lett. 36, 121–132. https://doi.org/10.1016/0012-821X(77)90193-5.

Pierrot, D., Lewis, E., Wallace, D.W.R., 2006. MS Excel program developed for CO2 system calculations. ORNL/CDIAC-105a. 10.3334/CDIAC/otg.CO2SYS_XLS_CDIAC105a.

Pinheiro, J., Bates, D., DebRoy, S., Sarkar, D., Core Team, R., 2017. nlme: linear and Nonlinear Mixed Effects Models.

Renforth, P., 2012. The potential of enhanced weathering in the UK. Int. J. Greenhouse Gas Control 10, 229–243. https://doi.org/10.1016/j.ijggc.2012.06.011.

Renforth, P., Henderson, G., 2017. Assessing ocean alkalinity for carbon sequestration. Rev. Geophys. 55, 636–674. https://doi.org/10.1002/2016RG000533.

Renforth, P., Pogge von Strandmann, P.A.E., Henderson, G.M., 2015. The dissolution of olivine added to soil: implications for enhanced weathering. Appl. Geochem. 61, 109–118. https://doi.org/10.1016/j.apgeochem.2015.05.016.

Rinder, T., von Hagke, C., 2021. The influence of particle size on the potential of enhanced basalt weathering for carbon dioxide removal - insights from a regional assessment. J. Clean. Prod. 315 https://doi.org/10.1016/j.jclepro.2021.128178.

Roland, M., Vicca, S., Bahn, M., Ladreiter-Knauss, T., Schmitt, M., Janssens, I.A., 2015. Importance of nondiffusive transport for soil CO2 efflux in a temperate mountain grassland. J. Geophys. Res. 120, 502–512. https://doi.org/10.1002/2014JG002788.

Rudnick, R.L., Gao, S., 2003. Composition of the continental crust. Treatise On Geochemistry.

Sarkar, S.R., 2021. Glacial Rock Flour: Its Characteristics and Enhanced Weathering. University of Copenhagen (PhD Thesis).

Shiklomanov, Rodda, J.C., 2004. World water resources at the beginning of the twenty-first century. Choice Rev. Online 41. https://doi.org/10.5860/choice.41-4063, 41-4063-41–4063.

Sims, R., Schaeffer, R., Creutzig, F., Cruz-Núñez, X., D'Agosto, M., Dimitriu, D., Figueroa Meza, M.J., Fulton, L., Kobayashi, S., Lah, O., McKinnon, A., Newman, P., Ouyang, M., Schauer, J.J., Sperling, D., Tiwari, G., 2014. Transport. In: Climate Change 2014: Mitigation of Climate Change. Contribution of Working Group III to the Fifth Assessment Report of the Intergovernmental Panel On Climate Change, in: Edenhofer, O., Pichs-Madruga, R., Sokona, Y., Farahani, E., Kadner, S., Seyboth, K. et al. (Eds.), . Cambridge University Press, United Kingdom and New York, NY, USA. 10.1007/978-3-319-12457-5_15.

Sørensen, N.K.K., Bülow-Olsen, A., 1994. Fælles arbejdsmetoder for jordbundsanalyser. Landbrugsministeriet Plantedirektoratet.

Strawn, D.G., Bohn, H.L., O'Connor, G.A., 2015. Soil Chemistry.

Taylor, L.L., Driscoll, C.T., Groffman, P.M., Rau, G.H., Blum, J.D., Beerling, D.J., 2021. Increased carbon capture by a silicate-treated forested watershed affected by acid deposition. Biogeosciences 18, 169–188. https://doi.org/10.5194/bg-18-169-2021.

Taylor, L.L., Quirk, J., Thorley, R.M.S.S., Kharecha, P.A., Hansen, J., Ridgwell, A., Lomas, M.R., Banwart, S.A., Beerling, D.J., Information, S., Taylor, L.L., Quirk, J., Thorley, R.M.S.S., Kharecha, P.A., Hansen, J., Ridgwell, A., Lomas, M.R., Banwart, S. A., Beerling, D.J., 2015. Enhanced weathering strategies for stabilizing climate and averting ocean acidification. Nat. Clim. Chang. 6, 402. https://doi.org/10.1038/nclimate2882.

ten Berge, H.F.M.M., van der Meer, H.G., Steenhuizen, J.W., Goedhart, P.W., Knops, P., Verhagen, J., 2012. Olivine weathering in soil, and its effects on growth and nutrient uptake in ryegrass (Lolium perenne L.): a pot experiment. PLoS ONE 7. https://doi.org/10.1371/journal.pone.0042098.

van Breemen, N., Mulder, J., Driscoll, C.T., 1983. Acidification and alkalinization of soils. Plant Soil 75, 283–308. https://doi.org/10.1007/BF02369968.

Vienne, A., Poblador, S., Portillo-Estrada, M., Hartmann, J., Ijiehon, S., Wade, P., Vicca, S., 2022. Enhanced weathering using basalt rock powder: carbon sequestration, co-benefits and risks in a mesocosm study with Solanum tuberosum. Front. Clim. 4, 869456 https://doi.org/10.3389/fclim.2022.869456.

Von Uexkull, H., Mutert, E., 1995. Global extent, development and economic impact of acid soils Author (s): h . R . von Uexküll and E . Mutert Source : plant and Soil, April (I) 1995, Vol . 171, No . 1, Selected papers from the THIRD INTERNATIONAL SYMPOSIUM ON PLANT-SOIL INTERACTI 171, 1–15.

Wang, J.G., Zhang, F.S., Cao, Y.P., Zhang, X.L., 2000. Effect of plant types on release of mineral potassium from gneiss. Nutr. Cycling Agroecosystems 56, 37–44. https://doi.org/10.1023/A:1009826111929.

Welch, S.A., Ullman, W.J., 1993. The effect of organic acids on plagioclase dissolution rates and stoichiometry. Geochim. Cosmochim. Acta 57, 2725–2736. https://doi.org/10.1016/0016-7037(93)90386-B.

White, P.J., 2013. Improving potassium acquisition and utilisation by crop plants. J. Plant Nutr. Soil Sci. 176, 305–316. https://doi.org/10.1002/jpln.201200121.

Wuest, S.B., 2015. Seasonal variation in soil bulk density, organic nitrogen, available phosphorus, and pH. Soil Sci. Soc. Am. J. 79, 1188–1197. https://doi.org/10.2136/sssaj2015.02.0066.

Wulffeld, J.L., 2021. Climate Mitigation and Food Production With Glacial Rock Flour. University of Copenhagen (PhD Thesis).

Yamaguchi, J., Tanaka, A., 1990. Quantitative observation on the root system of various crops growing in the field. Soil Sci. Plant Nutr. 36, 483–493. https://doi.org/10.1080/00380768.1990.10416917.

Yonemura, S.S., Yokozawa, M., Shirato, Y., Nishimura, S., Nouchi, I., 2009. Soil CO2 concentrations and their implications in conventional and no-tillage agricultural fields. J. Agric. Meteorol. 65, 141–149. https://doi.org/10.2480/agrmet.65.2.2.